Journal of Materials Science: Materials in Electronics
https://doi.org/10.1007/s10854-020-03722-y

Impact of weak ferromagnetism on the magnetocaloric properties of A-site-doped $PrMnO_3$ compound

Dipak Mazumdar[1] · Kalipada Das[2] · Pintu Sen[3] · I. Das[1]

Received: 25 April 2020 / Accepted: 1 June 2020

Abstract
Investigation of the magnetic ground state and magnetocaloric properties of the polycrystalline $Pr_{0.65}(Ca_{0.80}Sr_{0.20})_{0.35}MnO_3$ compound has been carried out in detail. In addition to the charge-orbital ordering and antiferromagnetic ordering transition, a weak ferromagnetic (FM) phase has been recognized from its temperature dependence of magnetization as well as from the change of magnetic entropies. The influence of such ferromagnetic phase on magnetocaloric effect have been examined properly in the presence of different magnetic fields. Moreover, a magnetic phase diagram, derived from the magnetic isotherms and magnetocaloric effect has been constructed to understand evolution of the weak ferromagnetic phase with external magnetic field at low temperature region.

1 Introduction

The phase coexistence scenario is a very trivial phenomena in the study of the colossal magnetoresistance (CMR) effect [1–7]. The competing nature between the metastable phases in presence of the external magnetic field and temperature initiates many intriguing physical properties like low field magnetoresistance, large magnetocaloric effect (MCE), metal–insulator transition. [8–14]. For a material having first-order magnetic transition, phase separation is governed by the disorder-mediated percolation between the equal density phases [15–18]. Due to the non-equilibrium nature of the competing phases, it is beneficial to tune the magnetic phase fraction by application of the small magnetic field. Regarding this context, it is worth mentioning that to realize the modification of the competing ground state, magnetocaloric effect (MCE) study may be treated as a powerful tool as reported earlier [19–23]. MCE is generally defined as the variation of the isothermal magnetic entropy change (ΔS) or adiabatic temperature change (ΔT_{ad}) of any magnetic material when it is subjected in the external magnetic field. From the fundamental and technological aspects, MCE for ferromagnetic or antiferromagnetic materials were extensively studied during previous few decades [24–28]. In this context, it is important to mention that magnetocaloric effect in the mixed phase magnetic materials also got an utmost attention to realize the evolution of the stability of different phases or phase transformation [23, 29, 30].

Doped perovskite manganite compounds are chemically represented by the general formula $A_{1-x}B_xMnO_3$ (A = trivalent elements and B = bivalent elements). Several intriguing physical properties have been achieved depending upon the choice of materials (A and B) and as well as on doping concentration 'x'. In case of the phase separated manganites, A = La, Pr and B = Ca–Sr and Ca–Ba were very well studied systems [24, 28, 31–36].

Regarding of our present study, a very brief discussion about the reported physical properties of $Pr_{0.65}\left(Ca_{1-y}Sr_y\right)_{0.35}MnO_3$ compound is given here. Based on the Sr doping concentration, Blake et al. had reported the magnetic phase diagram of the $Pr_{0.65}\left(Ca_{1-y}Sr_y\right)_{0.35}MnO_3$ compound, and it exhibits fascinating magnetic ground state [37]. According to their study, a sudden upturn in magnetization below $T = 200$ K was appeared for $y = 0.35$ and $y = 0.40$. However, the significant proportion of charge-ordered antiferromagnetic phase exists below $T = 200$ K for the $Pr_{0.65}(Ca_{0.65}Sr_{0.35})_{0.35}MnO_3$ compound. In addition to that, at low temperature ($T < 90$ K), an upturn in magnetization was appeared and this ferromagnetic phase fraction approached almost 100% at $T = 10$ K. It is important to mention that the

✉ Kalipada Das
kalipadadasphysics@gmail.com

[1] CMP Division, Saha Institute of Nuclear Physics, HBNI, 1/AF-Bidhannagar, Kolkata 700 064, India

[2] Department of Physics, Seth Anandram Jaipuria College, 10, Raja Naba Krishna Street, Kolkata 700005, India

[3] Variable Energy Cyclotron Centre, HBNI, 1/AF-Bidhannagar, Kolkata 700064, India

Published online: 08 June 2020

magnetization at low temperature for $y=0.20$, 0.25, and 0.30 concentration is lower than that for $y=0.75$ or $y=0.80$ compounds. Specifically, in case of the $Pr_{0.65}(Ca_{0.80}Sr_{0.20})_{0.35}MnO_3$ compound, the charge-ordered antiferromagnetic phase dominates over the whole temperature range. Moreover, the position of the present studied compound is near to the phase boundary (ferromagnetic and antiferromagnetic) region [37]. They showed lack of interest in the low temperature weak ferromagnetic phase of the compound. Considering those above mentioned facts, we have prepared the polycrystalline $Pr_{0.65}(Ca_{0.80}Sr_{0.20})_{0.35}MnO_3$ (PCSMO) compound and it's magnetic and magnetocaloric properties have been studied. The magnetic and magnetocaloric effect indicate that in addition to the charge-ordered and antiferromagnetic ordered state, a ferromagnetic phase is also present at the low temperature regime. The dynamics of this weak ferromagnetic phase with temperature and external magnetic field was described by constructing the magnetic phase diagram of this compound.

We used the well-known sol–gel method to prepare the polycrystalline PCSMO compound. There are also several other techniques namely electrodeposition, sputtering, etc. for the sample preparation. Sol–gel method is a very easy process to prepare oxide compounds and one can easily tune the doping concentration. Due to the well mixing of precursors at the molecular level, one can achieve better homogeneity and high purity compounds by utilizing sol–gel method. Apart from these benefits, sol–gel technique is a less energy consumption method where we also don't need any kind of special or expensive equipment. In contrast to that, the electrodeposition and sputtering method is very costly and time-consuming. Although these two methods have various advantages over sol–gel method as reported earlier in the literature [38–43].

2 Sample preparation and characterization

The well-established sol–gel chemistry route [33, 44, 45] has been employed to prepare the polycrystalline bulk $Pr_{0.65}(Ca_{0.80}Sr_{0.20})_{0.35}MnO_3$ (PCSMO) compound. In order to prepare the PCSMO compound, Pr_6O_{11}, $CaCO_3$, $SrCO_3$ and MnO_2 powders having purity greater than 99.99% have been used as raw materials along with oxalic acid, citric acid, and nitric acid as reacting agents. Stoichiometric amount of preheated rare-earth oxide and carbonates were converted into their corresponding nitrate solutions by adding concentrated nitric acid into the mixture and dissolved the whole solution into Millipore water. As the MnO_2 is insoluble in nitric acid, required amount of oxalic acid has been used in the solution. The mixture was then magnetically stirred for 30 min to get a homogenous mixture. To convert the solution into the gel form, desired amount of citric acid was added to the solution and set the solution for evaporation slowly at 80–90 °C in a water bath. After decomposing the gel at 200 °C, black powder was obtained. This powder was then reground, pelletized, and sintered at 1300 °C for 36 h to get the bulk polycrystalline PCSMO compound. The room temperature X-ray diffraction (XRD) spectrum of the powdered polycrystalline PCSMO compound reveals the single phase nature of the compound. The compound belongs to the *Pnma* space group having orthorhombic crystal structure. The DC magnetization measurements were carried out in a physical property measurement system (*M*/*S* Quantum Design Inc., USA).

3 Experimental results and discussion

In order to investigate the magnetic ground state of the compound, we have recorded magnetization data as a function of both temperature and magnetic field under various measuring protocols which are described as follows:

- *ZFCW* The virgin sample was cooled down to lowest desired temperature from room temperature in the absence of any external magnetic field and magnetization data were collected during warming cycle in the presence of desired static magnetic field.
- *FCC* Magnetic field was applied at the room temperature and the magnetization data were recorded during cooling of the sample.
- *FCW* The sample was cooled down to the desired temperature in presence of the static magnetic field and then magnetization data were recorded during warming cycle in presence of the same static magnetic field as applied during cooling.

Figure 1a shows the temperature dependence of magnetization measured under ZFCW and FCW protocols in presence of $H=500$ Oe magnetic field. Due to change of magnetic state (from paramagnetic to ferromagnetic), a discrete change in magnetization has been observed below 100 K. A huge divergence between ZFCW and FCW curves may be arisen due to the local anisotropic field generated from the FM/AFM clusters present in the system. These kind of magnetic clusters can be generated if the system is magnetically inhomogeneous or exhibiting the magnetic frustration [46, 47]. With increasing temperature, magnetization both in ZFCW and FCW protocols increases which may be due to the local ordering of rare-earth ions ($T<50$ K). In ZFCW protocol, a hump at $T\sim44$ K in magnetization curve is observed which manifested as blocking temperature (T_B) where magnetic moments are freeze in an energetically favored direction due to the local anisotropy of the system. Another strong hump has been observed in the magnetization curves which is due to the local charge ordering of Mn^{3+} and Mn^{4+} ions ($T\sim240$ K).

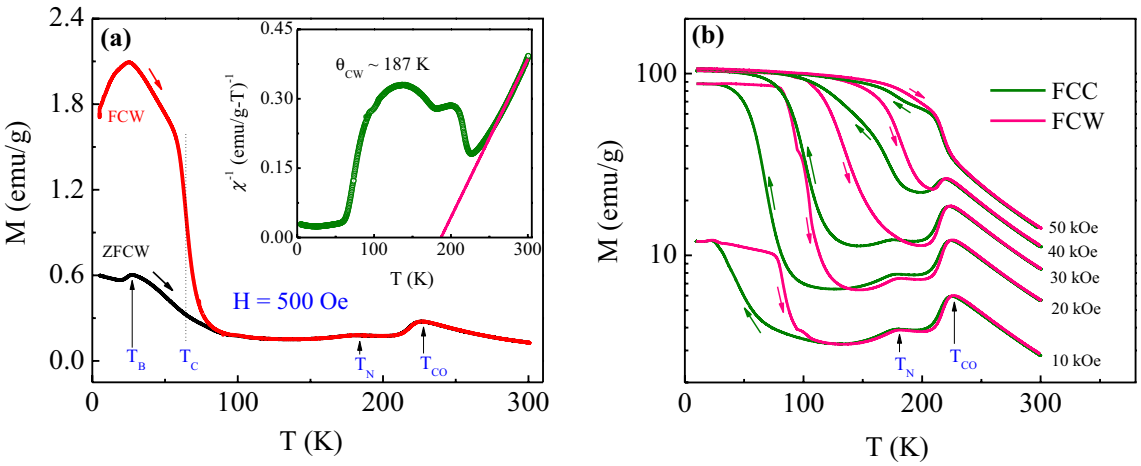

Fig. 1 **a** Magnetization as a function of temperature during ZFCW and FCW protocols in the presence of $H = 500$ Oe magnetic field. Inset shows the temperature dependence of inverse susceptibility plot (Olive) along with the paramagnetic Curie–Weiss fitted curve (red), **b** temperature dependence of magnetization recorded during field cooled cooling (FCC) (Olive) and during field cooled warming (FCW) (pink) protocols in presence of various external magnetic fields (Color figure online)

For better understanding the paramagnetic ground state of the compound, inverse susceptibility (χ^{-1}) as a function of temperature for $H = 500$ Oe has been plotted as shown in the inset of Fig. 1a. The inverse susceptibility (χ^{-1}) as a function of temperature shows interesting non-linear behavior. Using the Curie–Weiss (C–W) law of the form $\chi = C/(T - \theta_{CW})$ in the paramagnetic region, where $C = \mu_{eff}^2/3k$ is the Curie constant and θ_{CW} stands for paramagnetic Curie–Weiss temperature, the curve is fitted linearly in the paramagnetic region. The theoretical effective magnetic moment $\left((\mu_{eff})_{theo}\right)$ of the compound has been calculated using the following formula:

$$(\mu_{eff})_{theo} = \left[0.65 \times (\mu_{eff})^2_{Pr3+} + 0.65 \times (\mu_{eff})^2_{Mn3+} + 0.35 \times (\mu_{eff})^2_{Mn4+}\right]^{1/2}$$

where $(\mu_{eff})_{Pr3+}$, $(\mu_{eff})_{Mn3+}$, $(\mu_{eff})_{Mn4+}$ are calculated with the formula, $\mu_{eff} = g\{j(j+1)\}^{1/2}\mu_B$. The observed effective magnetic moment $\left((\mu_{eff})_{obs}\right)$ has been calculated from the linear fitting of χ^{-1} vs. T plot in the paramagnetic region (i.e., from Curie constant, $C = \mu_{eff}^2/3k$). The value of $(\mu_{eff})_{theo}$ is 5.4 μ_B/f. u. and the value of $(\mu_{eff})_{obs}$ is 7 μ_B/f. u.. Since $(\mu_{eff})_{obs} > (\mu_{eff})_{theo}$ and the positive value of $\theta_{CW} = 187$ K confirms the presence of short-range ferromagnetic interaction due to the formation of ferromagnetic/antiferromagnetic clusters in the paramagnetic region of the sample [48–50].

To observe the modification of magnetic ground state with temperature upon application of external magnetic field, magnetization as a function of temperature for various external magnetic fields have been recorded as shown in Fig. 1b. The data were collected in FCC and FCW protocols. One can clearly observe the increment of ferromagnetic fraction with increasing magnetic field strength. A strong thermal hysteresis present in between FCC and FCW curves corresponds to the first-order magnetic phase transition associated with it. Width of the thermal hysteresis drastically decreases (from $T_{width} = 47.7$ K at $H = 10$ kOe to $T_{width} = 1$ K at $H = 50$ kOe) with increasing magnetic field values. The charge-ordering temperature (T_{CO}) ~ 230 K remains unperturbed up to 40 kOe magnetic field. This charge-ordering state started melting upon application of 50 kOe magnetic field. Similarly, the antiferromagnetic ordering temperature (T_N) of Mn^{3+} and Mn^{4+} ions remains unchanged with increment of magnetic field strengths. An interesting feature has been noticed in the magnetization curves that the absence of low temperature ordering of rare-earth ions upon application of high magnetic fields. This may be due to the alignment of magnetic moments of rare-earth ions along the applied field direction which contributed ferromagnetically in the net magnetization value at low temperature region.

Magnetic field dependence of magnetization at $T = 5$ K has been recorded under ZFCW protocol during the field change of 0 $T \rightarrow 5$ $T \rightarrow 5$ $T \rightarrow 5$ T as shown in Fig. 2. With increasing magnetic field, magnetization increases linearly due to the dominating nature of the canted AFM ground state. This canted AFM ground state is unstable, and further increment of magnetic field above 20 kOe help to convert this canted AFM ground state into a FM stable state which remains constant upon subsequent of field cycling as shown in the inset of Fig. 2. This represents the system undergoes a

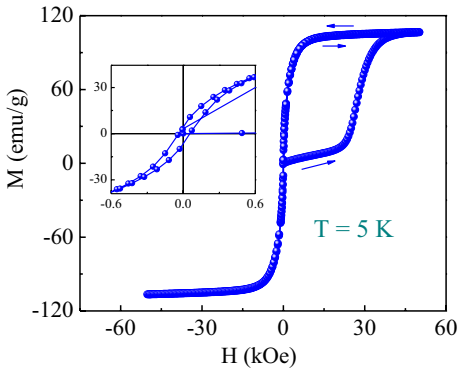

Fig. 2 Magnetization as a function of external magnetic field at $T = 5$ K. Inset shows the enlarged view of the magnetization at low field region

metamagnetic (AFM → FM) like first-order magnetic transition upon application of magnetic field.

In general, this kind of metamagnetic transition is temperature-dependent. To calculate the required critical magnetic fields (H_C) at various temperatures, we have measured various temperature-dependent magnetization curves under ZFCW protocol as shown in Fig. 3a. For the sake of clarity, we have shown *M–H* curves for selected temperatures. Below a certain temperature (T_{CO}), magnetization increases linearly in the low field region, and after that, a metamagnetic transition takes place and it reaches its saturation value. This S-shaped nature of *M–H* curves (at low temperature) may be attributed to the fact of inhomogeneous metastable state in the presence of quenched disorder as reported by Sarkar et al. [51]. Above T_{CO}, magnetization increases almost linearly with magnetic field corresponding to the paramagnetic state of the system.

In order to confirm the nature of magnetic phase transition, Arrott plots (M^2 vs. H/M) [52] have been constructed using the isothermal magnetization curves as shown in Fig. 3a. Using Banerjee criterion [53] on the slopes of Arrott plots, one can easily explain the order of magnetic phase transition. If the slope of M^2 vs. H/M curves is positive, then the transition associated with the system is second order in nature and vice versa. In case of our PCSMO compound, the slope of the M^2 vs. H/M curves is negative in the low field region implying that the magnetic transition associated with the system is a conventional first-order type as shown in Fig. 3b.

The change of magnetic entropy (ΔS) upon application of magnetic fields can be calculated using Maxwell's thermodynamic relation [54] as given by

$$\Delta S = \int_0^H \frac{dM}{dT} dH \tag{1}$$

The variation of the magnetic entropy change as a function of temperature is given in Fig. 4. The signature of different magnetic phase transitions has been clearly reflected in the $-\Delta S$ vs. T plots. With decreasing temperature, the change of magnetic entropy ($-\Delta S$) values alters its sign which can be incorporated as inverse magnetocaloric effect (IMCE). The peak temperature value of IMCE corresponds to the local charge-orbital ordering of Mn^{4+} and Mn^{3+} ions. With further lowering of temperature, $-\Delta S$ shows a positive value which indicates the ferromagnetic nature of the already converted ground state of the compound. At low temperature, the numerical value of the magnetic entropy change ($-\Delta S$) drastically increases after it crosses the critical field value (~ 20 kOe) of metamagnetic phase transition. Moreover, at very higher magnetic field values, the change of magnetic entropy ($-\Delta S$) tends to saturate.

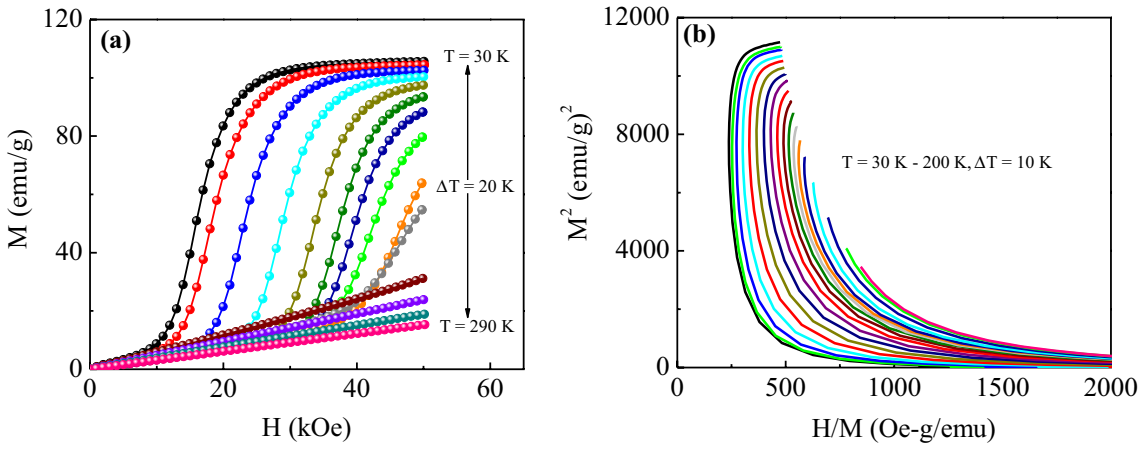

Fig. 3 **a** External magnetic field-dependent magnetization of PCSMO compound at some selected temperatures, **b** Arrott plot (M^2 vs. H/M) of the PCSMO compound at different temperatures, indicates the first-order nature of the magnetic phase transition

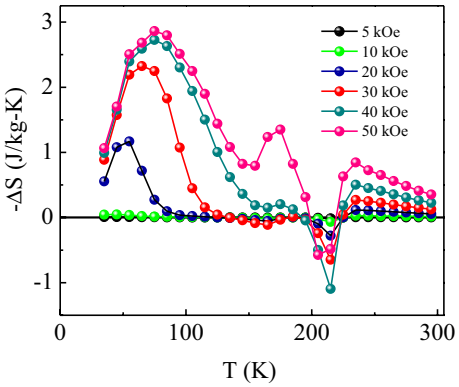

Fig. 4 Isothermal magnetic entropy change $(-\Delta S)$ as a function of temperature at different external magnetic fields

The field-induced metamagnetic phase transition is very sensitive to the temperature. The critical magnetic field (H_C) values and the critical temperature (T_C) are extracted from the derivatives of isothermal magnetization curves and the temperature-dependent magnetic entropy change curves, respectively. These kind of extraction of critical parameters has been shown in Fig. 5. Both the derivatives of the magnetization and magnetic entropy change exhibits metamagnetic transition almost in the same magnetic field when the temperatures are very close to each other. By extracting the values of critical magnetic field at different temperatures from the magnetization as well

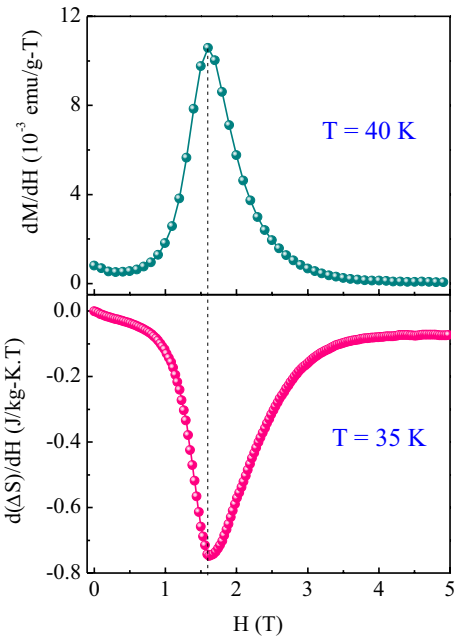

Fig. 5 Magnetic field-dependent derivative of magnetization (upper panel) and magnetic entropy changes (lower panel) at very close temperature

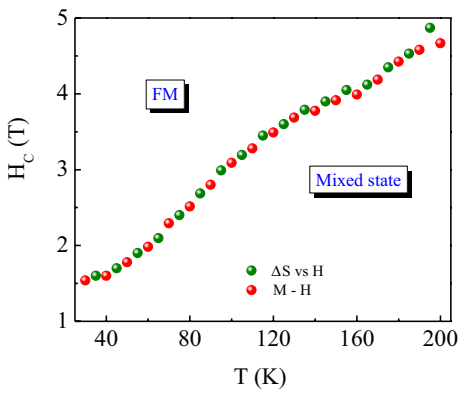

Fig. 6 Magnetic phase diagram of the low temperature weak ferromagnetic phase of PCSMO compound constructed from the magnetization and magnetocaloric effect

as magneto caloric effect study, we have constructed the magnetic phase diagram (MPD) of the compound. The generated MPD is depicted in Fig. 6. MPD of the compound indicates that the critical magnetic field increases with increasing the temperature.

4 Conclusions

To summarize, we have reported the magnetic and magnetocaloric effect of polycrystalline PCSMO compound as prepared using standard sol–gel method. In addition to the charge-orbital and antiferromagnetic ordering, a weak ferromagnetic phase was identified which is dominated specially at low temperature region. Moreover, the system undergoes a metamagnetic-like phase transition upon application of high magnetic field ($H \sim 20$ kOe) at low temperature region. This confirms the metastable magnetic nature of its ground state (canted AFM state). The dynamics of the low temperature weak ferromagnetic phase were studied through the construction of the magnetic phase diagram using the extracted critical parameters from the magnetization and magnetocaloric effect study.

Acknowledgements The work was supported by Department of Atomic Energy (DAE), Govt. of India.

Compliance with ethical standards

Conflict of interest The authors declare that they have no conflict of interest.

References

1. Y. Tokura, *Colossal Magnetoresistive Oxides* (Gordon and Breach Science Publishers, The Netherlands, 2000)
2. E. Dagotto, Science **309**, 257 (2005)
3. N. Mathur, P. Littlewood, Phys. Today **56**(1), 25 (2003)
4. M.H. Phan, M.B. Morales, N.S. Bingham, H. Srikanth, C.L. Zhang, S.W. Cheong, Phys. Rev. B **81**, 094413 (2010)
5. J. Tao, D. Niebieskikwiat, M. Varela, W. Luo, M.A. Schofield, Y. Zhu, M.B. Salamon, J.M. Zuo, S.T. Pantelides, S.J. Pennycook, Phys. Rev. Lett. **103**, 097202 (2009)
6. Y. Tokura, Rep. Prog. Phys. **69**, 797 (2006)
7. W. Kundhikanjana, Z. Sheng, Y. Yang, K. Lai, E.Y. Ma, Y.-T. Cui, M.A. Kelly, M. Nakamura, M. Kawasaki, Y. Tokura, Q.C. Tang, K. Zhang, X.X. Li, Z.-X. Shen, Phys. Rev. Lett. **115**, 265701 (2015)
8. Z.B. Guo, J.R. Zhang, H. Huang, W.P. Ding, Y.W. Du, Appl. Phys. Lett. **70**, 904 (1996)
9. Y. Moritomo, A. Asamitsu, H. Kuwahara, Y. Tokura, Nature **380**, 141 (1996)
10. M. Uehara, S. Mori, C.H. Chen, S.W. Cheong, Nature **399**, 560 (1999)
11. A. Biswas, T. Samanta, S. Banerjee, I. Das, Appl. Phys. Lett. **92**, 012502 (2008)
12. K.A. Gschneidner Jr., V.K. Pecharsky, A.O. Tsokol, Rep. Prog. Phys. **68**, 1479 (2005)
13. R.Y. Gu, C.S. Ting, Phys. Rev. B **65**, 214426 (2002)
14. Y. Lu, J. Klein, F. Herbstritt, J.B. Philipp, A. Marx, R. Gross, Phys. Rev. B **73**, 184406 (2006)
15. J. Burgy, E. Dagotto, M. Mayr, Phys. Rev. B **67**, 014410 (2003)
16. O. Gutfleisch, T. Gottschall, M. Fries, D. Benke, I. Radulov, K.P. Skokov, H. Wende, M. Gruner, M. Acet, P. Entel, M. Farle, Philos. Trans. R. Soc. A **374**, 20150308 (2016)
17. L. Zhang, C. Israel, A. Biswas, R.L. Greene, A. de Lozanne, Science **298**, 805 (2002)
18. R. Rawat, P. Kushwaha, D.K. Mishra, V.G. Sathe, Phys. Rev. B **87**, 064412 (2013)
19. R. M'nassri, Phase Trans. **90**(7), 687 (2016)
20. H. Zhu, C. Xiao, H. Cheng, F. Grote, X. Zhang, T. Yao, Z. Li, C. Wang, S. Wei, Y. Lei, Y. Xie, Nat. Commun. **5**, 3960 (2014)
21. D.M. Polishchuk, YuOT Polishchuk, E. Holmgren, A.F. Kravets, A.I. Tovstolytkin, V. Korenivski, Phys. Rev. Mater. **2**, 114402 (2018)
22. F. Cugini, G. Porcari, S. Fabbrici, F. Albertini, M. Solzi, Philos. Trans. R. Soc. A **374**, 20150306 (2016)
23. D. Mazumdar, K. Das, S. Roy, I. Das, J. Magn. Magn. Mater. **497**, 166066 (2020)
24. A.M. Tishin, Y.I. Spichkin, *TheMagnetocaloric Effect and its Applications* (Institute of Physics Publishing, Bristol and Philadelphia, 2003)
25. H. Wada, Y. Tanabe, M. Shiga, H. Sugawara, H. Sato, J. Alloys and Compd. **316**, 245 (2001)
26. J. Liu, T. Gottschall, K.P. Shokov, J.D. Moore, O. Gutfleisch, Nat. Mater. **11**, 620 (2012)
27. A.O. Pecharsky, K.A. Gschneidner Jr., V.K. Pecharsky, J. Appl. Phys. **93**, 4722 (2003)
28. M.H. Phan, S.C. Yu, J. Magn. Magn. Mater. **308**, 325 (2007)
29. T. Paramanik, T. Samanta, R. Ranganathan, I. Das, RSC Adv. **5**, 47860 (2015)
30. K. Das, I. Das, J. Magn. Magn. Mater. **439**, 328 (2017)
31. M.B. Salamon, M. Jaime, Rev. Mod. Phys. **73**, 583 (2001)
32. C.N.R. Rao, R. Raveau (eds.), *Colossal Magnetoresistance, Charge Ordering and Related Properties of Manganese Oxides* (World Scientific, Singapore, 1998)
33. K. Das, P. Dasgupta, A. Poddar, I. Das, Sci. Rep. **6**, 20351 (2016)
34. S. Jin, T.H. Tiefel, M. McCormack, R.A. Fastnacht, R. Ramesh, L.H. Chen, Science **264**, 413 (1994)
35. S. Banik, K. Das, I. Das, RSC Adv. **7**, 16575 (2017)
36. N.S. Bingham, M.H. Phan, H. Srikanth, M.A. Torija, C. Leighton, J. Appl. Phys. **106**, 023909 (2009)
37. G.R. Blake, L. Chapon, P.G. Radaelli, D.N. Argyriou, M.J. Gutmann, J.F. Mitchell, Phys. Rev. B **66**, 144412 (2002)
38. H. Kockar, M. Alper, H. Topcu, Eur. Phys. J. B **42**, 497 (2004)
39. T. Sahin, H. Kockar, M. Alper, J. Magn. Magn. Mater. **373**, 128 (2015)
40. H. Kockar, M. Alper, H. Kurua, T. Meydan, J. Magn. Magn. Mater. **304**, 736 (2006)
41. H. Kockar, J. Supercond. **17**, 4 (2004)
42. H. Kockar, T. Meydan, Phys. B **321**, 124 (2002)
43. T. Meydan, H. Kockar, Eur. Phys. J. B **24**, 457 (2001)
44. A. Biswas, I. Das, Phys. Rev. B **74**, 172405 (2006)
45. A. Biswas, I. Das, C. Majumdar, J. Appl. Phys. **98**, 124310 (2005)
46. T.L. Phan, T.A. Ho, T.V. Manh, N.T. Dang, C.U. Jung, B.W. Lee, T.D. Thanh, J. Appl. Phys. **118**, 143902 (2015)
47. D.N.H. Narn, R. Mathieu, P. Nordblad, N.V. Khiem, N.X. Phuc, Phys. Rev. B **62**, 1027 (2000)
48. D. Mazumdar, K. Das, I. Das, J. Magn. Magn. Mater. **502**, 166507 (2020)
49. M.M. Saber, M. Egilmez, A.I. Mansour, I. Fan, K.H. Chow, J. Jung, Phys. Rev. B **82**, 172401 (2010)
50. M.B. Salamon, P. Lin, S.H. Chun, Phys. Rev. Lett. **88**, 197203 (2002)
51. P. Sarkar, S. Arumugam, P. Mandal, A. Murugeswari, R. Thiyagarajan, S. Esaki Muthu, D. Mohan Radheep, C. Ganguli, K. Matsubayshi, Y. Uwatoko, Phys. Rev. Lett. **103**, 057205 (2009)
52. A. Arrott, Phys. Rev. **108**, 1394 (1957)
53. S.K. Banerjee, Phys. Lett. **12**, 16 (1964)
54. T. Hashimoto, T. Numasawa, M. Shino, T. Okada, Cryogenics **21**, 647 (1981)